Suitability and Utility of Computational Analysis Tools: Characterization of Erythrocyte Parameter Variation

R.E. Altenbaugh, K.J. Kauffman, J.S. Edwards

Pacific Symposium on Biocomputing 8:104-115(2003)

SUITABILITY AND UTILITY OF COMPUTATIONAL ANALYSIS TOOLS: CHARACTERIZATION OF ERYTHROCYTE PARAMETER VARIATION

R. E. ALTENBAUGH[*], K. J. KAUFFMAN[*], J. S. EDWARDS
Dept of Chemical Engineering, University of Delaware
Newark, DE 19716 USA
[*]Contributed equally

Systems engineering can provide insights into multivariate regulatory networks and pooling in complex biological networks that cannot be fully interpreted through experiments alone. Herein, we analyzed the use of phase planes, modal and time-lagged correlation (TLC) analyses of the human erythrocyte to explore the utility of these techniques for understanding the effect of single parameter changes on the behavior of a metabolic network. Specifically, several parameters in key regulatory steps in erythrocyte glycolysis, Rapoport-Leubering bypass, pentose phosphate pathway, adenosine metabolism, and membrane transport were perturbed. The most sensitive parameters were identified based on the steady-state metabolite concentration changes and were explored further. Modal analysis identified relevant time scales for each parameter change. These time scales were further explored using phase plane and TLC analyses. Phase plane and TLC both inferred pooling changes, while TLC also identified changes in the regulatory network structure that resulted from various parameter changes. Each method has strengths and weaknesses for exploring and gaining insight into complex biological networks.

1. Introduction

Biological system models can serve as suitable benchmarks for the development and comparison of analysis tools to study metabolic and regulatory networks. The modified Joshi and Palsson model of human Red Blood Cell (RBC) metabolism[1-6] is the most complete dynamic model of a cell that is currently available. Furthermore, the RBC model is relatively simple compared to other cellular networks, consisting of 44 enzymatic reactions and membrane transport systems describing the dynamics of 34 metabolites and ions. Although the RBC metabolic model is not complete in every aspect, it entails many of the issues expected to arise in the normal behavior of complex cellular systems such as nonlinear enzyme kinetics, multilayer feedback mechanisms, competing time scale effects, and pathway regulation.

Biological network models are primarily analyzed using purely linear techniques such as metabolic control analysis (MCA). In MCA, sensitive enzymes are identified by the steady-state impact of minute enzyme parameter changes.[7] Such techniques miss nonlinear feedback and regulatory effects that can significantly alter the underlying dynamics. Time-lagged correlation (TLC) analysis is a more general technique that measures nonlinear dynamic effects through random system

disturbances selected to excite those dynamics. Arkin and Ross used TLC as the basis for a correlation metric construction analysis which takes the strongest correlations between metabolites, converts those correlations into a distance metric, and then projects those distances into an optimized 2D representation. The idea behind this work was that the 2D projection gave insight into the relative differences between metabolites.[8,9] However, in creating a simplified 2D projection, much of the TLC information is ignored. This necessitates alternative techniques.

Kauffman and coworkers explored the use of modal analysis, physiological pooling, phase plane analysis, and TLC for improved understanding of the dynamics of RBC metabolism.[10] These techniques are data intensive, and, at present, a full *in vivo* comparison is not feasible for large scale systems. Therefore, the RBC model provided sample data sets that allowed for a comparison of the techniques, evaluation of requirements and limitations of each technique, and exploration of experimental issues that may arise. However, Kauffman *et al.* did not explore the sensitivity of the results to variations in the kinetic parameters in the model—corresponding to discrete differences in metabolic networks.

The present work explores the ability of phase plane analysis and TLC to identify and characterize differences arising from single parameter changes in a complex metabolic network (corresponding to SNPs). Modal analysis was used to identify dynamic intervals of interest, thus focusing the data analysis techniques on time-scales of interest.

The RBC model used in this study modeled each of 34 metabolites using a series of differential-algebraic equations coded in FORTRAN. The resulting equations were solved using D02NDF and associated routines from the NAG™ Library.[11] This solver is ideally suited for sparse, stiff systems that undergo a series of dramatic environmental changes, including biological systems such as the RBC. The rate parameters were as previously published.[3,10] The complete code is available for download at http://epicurus.che.udel.edu/downloads/.

1.1 Parameter Sensitivity and Alterations:

RBC model parameters were altered systematically one parameter at a time. Individual parameters were increased and decreased (ΔP_j) until the steady-state (SS^{Δ}) of the new system differed significantly from the nominal case (SS^{o}), as described by the normalized sum squared differences between the two steady-states. Parameter changes were selected so the sum squared difference between the steady-states approached 1. For most changes, this allowed the system to be altered without risking instability when energy loads or random disturbances were applied.

The sensitivity (Ψ) was numerically defined as the sum squared fractional difference of the steady-states (Γ) scaled by the corresponding parameter change:

$$\Psi_j^{\pm} = \frac{1}{\Delta P_j^{\pm}} \sum_{i=1}^{34} \left(\frac{SS_i^o - SS_i^{\Delta}}{SS_i^o} \right)^2$$

1.2 Analysis Techniques

Phase Plane Analysis: Phase planes plotted the concentrations of two metabolites, each parameterized with respect to time, against each other.[12] The phase plane analysis worked well for monitoring the changes in response to a step change in the environment of the metabolic network. In this study, one of three zero order step changes were made, simulating nonspecific changes in the usage efficiency of cellular currencies: 2.0 mM/h ATP load, 0.15 mM/h redox load, and a combination of 1.0 mM/h ATP load and 0.075 mM/h redox load. The strengths of the combined loads were smaller than the individual loads to prevent physiologically insignificant steady-states.[5] The effects of the three loads were followed for up to 310 h as the modeled cells responded from the steady-state identified following the parameter change to a new steady-state corresponding to the presence of the load(s). Phase planes constructed over time scales of interest were analyzed to identify pools of metabolites which had strong linear tendencies by computing a regression coefficient and the slope of the resulting best-fit line. Species with high regression coefficients and conserved, positive slope values were pooled together as equilibrium pools where the equilibrium constant was related to the slope of the best-fit line.[10]

Time-Lagged Correlation Analysis: A correlation array R, was constructed:

$$\mathbf{R}(\tau) = \left(r_{ij}(\tau) = \frac{\frac{1}{n} \sum_{k=1}^{n-\tau} \left(x_i(k) - \bar{x}_i \right) \left(x_j(k+\tau) - \bar{x}_j \right)}{\left[S_{ii} S_{jj} \right]^{0.5}} \right)$$

where S_{ii} was the variance and $\bar{x}_i$ was the mean value of the uniformly sampled dataset $x_i(t)$. Values of $r_{ij}(\tau)$ range from -1 to 1, where values approaching -1 indicate two datasets perfectly anti-correlated with a delay of τ time steps; values approaching 1 indicate two datasets perfectly correlated with a delay of τ time steps; and values approaching 0 indicate two datasets statistically unrelated at a delay of τ time steps. Pools of metabolites were identified by correlations stronger than 0.985 and peaking at zero lag.[10] Other peaks in correlation were used to infer potential connectivity and regulation.

TLC required that appropriate perturbations were applied to ensure persistent excitation of the network. Persistent excitation was achieved by application of truncated Gaussian perturbations for two extracellular concentrations (mM): glucose (GLU, μ=5, σ^2=2), hypoxanthine (HX, μ=10^{-5}, σ^2=10^{-5}) and three currency loads (mM/h): NADH (μ=0.1, σ^2=0.033), GSH (μ=0.1, σ^2=0.033), and ATP (μ=0.1,

σ^2=0.033). Each input sequence was truncated to prevent negative concentrations or generation terms. Data were collected with a sampling frequency of 2 samples per perturbation and a fixed frequency of random perturbations for 2001 measurements. The resulting data were analyzed with TLC, which provided similar results to phase plane analysis with three key distinctions. First, TLC directly accounted for delayed effects whereas phase plane analysis did not. Second, TLC identified poolings and correlations based on deviations from the mean value whereas phase planes analyzed the absolute concentrations. Finally, whereas phase planes provided insight into how the metabolite moved from one steady-state to the next, TLC analyzed behavior with respect to persistent excitation.

Modal Analysis: A third technique used for analysis of the effects of various alterations was modal analysis. Modal analysis identified inherent time scales within the system and whether those time scales contained oscillatory contributions. Modal analysis first calculates the Jacobian matrix by multiplying the stoichiometric matrix with the vector of the gradient of the rate equations linearized about a desired steady-state. The Jacobian matrix was diagonalized as $J=M\Lambda M^{-1}$. The actual concentrations were transformed into a vector of independent modes, defined as $m=M^{-1}x$. Each mode moved on a characteristic time constant, defined as the negative inverse of the eigenvalue corresponding to the eigenvector of the Jacobian.[13] Significant changes in the time constants focused the TLC and phase plane analyses to interesting dynamic regions. While the modal analysis saved a significant amount of effort and time, it was not required for the other analyses (phase planes and TLC) which are data driven techniques and do not require an underlying model.

2. Results

Table I summarizes the resulting sensitivities for each parameter alteration. To prevent physiologically insignificant steady-states, parameters were decreased no more than 90% and increased no more than 1000 fold from their nominal values. When parameters changes within this region led to insignificant Ψ, the parameters were classified as "insensitive". Each of the remaining parameter changes were analyzed using the three methods described above. Parameter alterations were classified into four categories, depending on which component of RBC metabolism was affected: glycolysis, pentose-phosphate pathway (PPP), adenosine metabolism, and membrane transport. Each category is explored in greater detail.

2.1 Glycolytic Pathway

The glycolytic pathway is thought to be rate controlled by five enzymes: hexokinase (HK), phosphofructokinase (PFK), pyruvate kinase (PK), diphosphoglycerate (DPG)

mutase (DPGM) and DPG phosphatase (DPGase).[3] The first three enzymes in this group are part of glycolysis, while the last two constitute the Rapoport-Leubering bypass, a feature specific to the RBC. For each of the core glycolytic enzymes, three parameters were changed: activity constant (V_{max}), ATP inhibition constant ($K_{m,ATP}$) or MgATP inhibition constant ($K_{m,MgATP}$) as appropriate, and substrate inhibition constant ($K_{m,Substrate}$).

Glycolytic parameter alterations manifested themselves as one of three phenotypes: increased ATP levels, decreased ATP levels, no significant effect (see Table II). TLC provided the most insight into glycolytic changes, typically manifested as pooling changes (Table III). Both the identified pools and the ATP phenotype were the same for changes in the V_{max} parameter of HK and PK. Increasing either of these two parameters led to sedoheptulose-7-phosphate (S7P) moving independently from the ribulose-5-phosphate (RU5P) pool. This common behavior was observed for several other parameter changes as well. Decreasing V_{max} for either HK or PK combined the 5-phosphoribosyl-1-pyrophosphate (PRPP) and RU5P pools. Almost all of the explored changes to the model parameters dissolved HX and inosine (INO) from the adenosine (ADO)/AMP/HX/INO pool. Under glucose limiting conditions (i.e., $K_{m,GLC}$ increased for HK), the RBC became more sensitive to perturbations, particularly ATP loads. Interestingly, this increased load sensitivity does not correspond to a significant change in the system steady-state. The largest $K_{m,GLC}$ change permitting stable application of the loads was $\Delta P^{+}=8.0$ ($\Gamma=0.27$). No other parameters explored demonstrated this type of sensitivity.

Other alterations to HK inhibition resulted in unique system changes. TLC revealed that increasing $K_{m,MgATP}$ or decreasing $K_{m,GLC}$ caused 6-phosphoglyconate (GO6P) to no longer pool with glucose-6-phophate (G6P) and fructose-6-phosphate (F6P). Under either parameter change, GO6P became less correlated with glycolysis while remaining highly correlated with the $NADP^{+}$/GSH pool in the PPP (Fig. 1). This resulted from PPP moving independent of glycolysis on the time scale explored.

2.2 Pentose Phosphate Pathway (PPP)

Three enzymes were perturbed in the PPP: G6P dehydrogenase (G6PDH), 6-phosphogluconolactonate (GL6P) dehydrogenase (GL6PDH), and glutathione oxidase (GSHR). The first two reactions were reversible: their equilibrium constants were shifted by changing the ratios of their forward and reverse kinetic constants. Changes in G6PDH and GL6PDH parameters only significantly affected levels of GO6P and $NADP^{+}$. Both G6PDH and GL6PDH were found to be insensitive to changes in their respective inhibition constants. G6PDH was found to be highly sensitive to shifts in equilibrium whereas GL6PDH was not. G6PDH equilibrium shifts were analogous to strong changes in V_{max} (G6PDH). Decreasing G6PDH activity decreased $NADP^{+}$ and GO6P without affecting 6-phosphogluconolactone

Table I: Parameter alterations and observed sensitivity. (A) glycolysis, (B) pentose phosphate pathway, (C) adenosine metabolism, and (D) transport in the RBC. Ψ=IS denotes insensitive parameters, IC denotes intracellular, XC denotes extracellular. *Γ=0.28 was used to prevent metabolic crash for HK.

(A)	HK	PFK	PK
V_{max}	Ψ^-=11.11, Ψ^+=10.00	Ψ^-=IS, Ψ^+=0.22	Ψ^-=2.86, Ψ^+=0.88
$K_{m,ATP}$	Ψ^-=IS, Ψ^+=0.95 (MgATP)	Ψ^-=1.67, Ψ^+=0.91	Ψ^-=1.89, Ψ^+=0.17
$K_{m,Substrate}$	Ψ^-=IS, *Ψ^+=0.034	Ψ^-=1.56, Ψ^+=IS	Ψ^-=2.04, Ψ^+=1.79
(B)	G6PDH	GL6PDH	GSHR
V_{max}	Ψ^-=1.30, Ψ^+=IS	Ψ^-=2.08, Ψ^+=IS	Ψ^-=1.79, Ψ^+=1.54
K_m	Ψ^-=IS, Ψ^+=0.01	Ψ^-=IS, Ψ^+=0.26	Not applicable
⇄	(→G6P), (→GL6P) Ψ^-=9.10, Ψ^+=8.33	(→GO6P), (→RU5P) Ψ^-=IS, Ψ^+=0.17	Not applicable
(C)	Adenosine Kinase (ADK)	ATPase	AMPase
V_{max}	Ψ^-=IS, Ψ^+=IS	Ψ^-=4.54, Ψ^+=4.00	Ψ^-=2.70, Ψ^+=2.00
⇄	(→ ATP), (→ ADP) Ψ^-=2.50, Ψ^+=2.08	Not applicable	Not applicable
(D)	AEX	K^+ Leak	Na^+ Leak
V_{max}	Ψ^-=1.67, Ψ^+=0.01	Ψ^-=1.72, Ψ^+=IS	Ψ^-=2.08, Ψ^+=1.82
$K_{m, XC}$	Ψ^-=2.70, Ψ^+=1.11	Ψ^-=1.45, Ψ^+=IS	Ψ^-=IS, Ψ^+=0.20
$K_{m, IC}$	Ψ^-=2.38, Ψ^+=2.38	Ψ^-=IS, Ψ^+=0.05	Ψ^-=1.22, Ψ^+=0.50
	Na^+/K^+ Pump		
K^+ Inhibitor	Ψ^-=IS, Ψ^+=IS		
$K_{m,Na}$	Ψ^-=IS, Ψ^+=3.65		
$K_{m,ATP}$	Ψ^-=IS, Ψ^+=2.38		

Table II: Summary of glycolytic parameter manipulations resulting in observed phenotype..

Phenotype	Changes of parameters in glycolysis pathway
ATP Decrease	↓ V_{max} (HK), ↑ $K_{m,MgATP}$ (HK), ↓ $K_{m,ATP}$ (PFK), ↓ V_{max} (PK), ↑ $K_{m,PEP}$ (PK), ↓ $K_{m,ATP}$ (PK)
ATP Increase	↑ V_{max} (HK), ↓ $K_{m,MgATP}$ (HK), ↓ $K_{m,F6P}$ (PFK), ↑ V_{max} (PFK), ↑ V_{max} (PK), ↓ $K_{m,PEP}$ (PK), ↑ $K_{m,ATP}$ (PK), ↑ $K_{m,ATP}$(PFK)
No noticeable effects	$K_{m,MgATP}$ (PFK), $K_{m,GLC}$ (HK)

Table III: Time-lagged correlation of glycolytic pathway reveals changing pools.

	Pools	
Nominal	G6P/F6P/G06P FDP/GAP/DHAP PG3/PG2/PEP R5P/RU5P/X5P/S7P/R1P	AD0/AMP/HX/INO NADPH/GSH PYR|NADH ADE|PRPP
Decreased ATP		
↓ V_{max} (HK,PK)	ADE|PRPP combine with (R5P/RU5P/X5P/S7P/R1P)	AD0/AMP/~~HX/INO~~
↓ $K_{m,ATP}$ (PFK)	R5P/RU5P/X5P/R1P/~~S7P~~	AD0/AMP/~~HX/INO~~
Increased ATP		
↑ V_{max} (HK,PK)	R5P/RU5P/X5P/R1P/~~S7P~~	AD0/AMP/~~HX/INO~~
↓ $K_{m,PEP}$ (PK)	R5P/RU5P/X5P/R1P/~~S7P~~	AD0/AMP/~~HX/INO~~
No effect on system		
↑ $K_{m,MgATP}$ (HK)	G6P/F6P/~~G06P~~	AD0/AMP/~~HX/INO~~

Table IV: Major changes in steady-state metabolite concentrations arising from altered transport kinetics.

Parameter change	Steady-state levels
ADE Tx: $\downarrow V_{max}$, $\downarrow K_m$(ADE ext), $\uparrow K_m$(ADE int)	↓ADE (38%), ↑PRPP(100%)
K^+ Leak: $\downarrow V_{max}$, $\downarrow K_m(K^+$ ext), $\uparrow K_m(K^+$ int)	$\uparrow K^+$(103%)
Na^+ Leak: $\downarrow V_{max}$, $\uparrow K_m(Na^+$ ext), $\downarrow K_m(Na^+$ int)	$\downarrow Na^+$(58%), $\downarrow K^+$(40%), $\downarrow NADP^+$(19%), ↑G6P(30%), ↑ATP(10%), ↑RU5P(13%), ↑PRPP(28%)
Na^+/K^+ ATPase Pump: $\uparrow K_m(Na^+)$, $\uparrow K_m$(ATP)	$\downarrow K^+$(68%),↑ Na^+(78%), ↑G6P(23%), ↑ATP(8%),

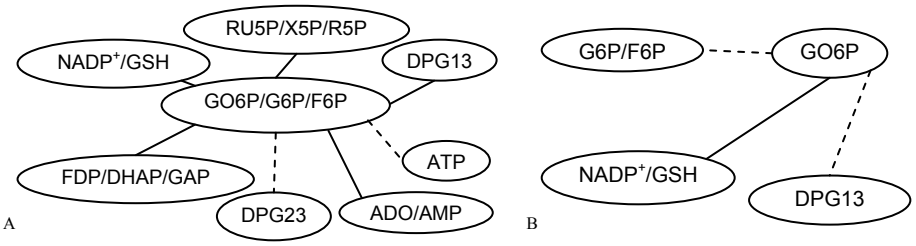

Figure 1: System connectivity to GO6P metabolite using TLC. (─) strong correlation (r_{ij} >0.80); (--) weak correlation ($0.05 \leq r_{ij} \leq 0.80$); A. Normalized system, B. Increased $K_{m,GLC}$ in HK.

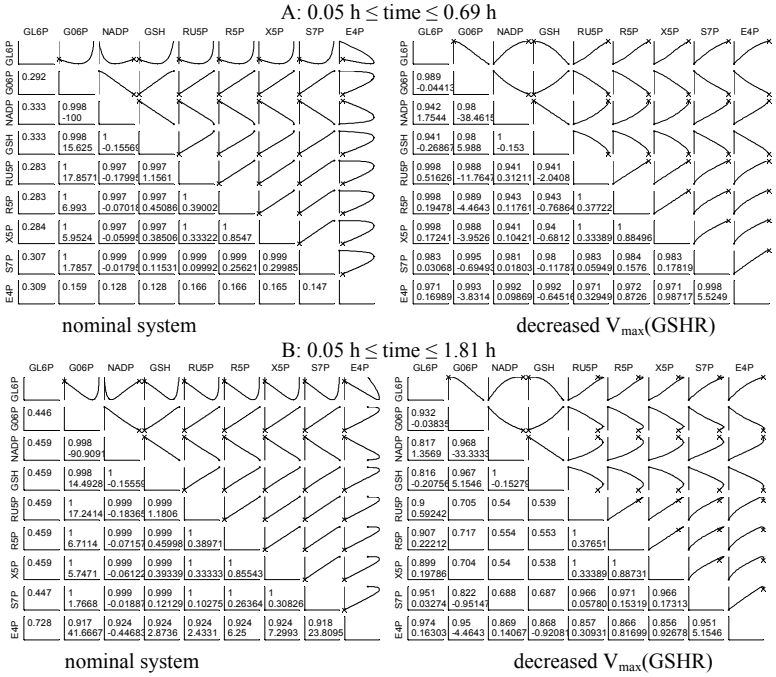

Figure 2: Phase planes for nominal and perturbed case. Manipulation of maximum rate of GSHR: (x) denotes starting point, (.) denotes ending point. The numbers in the lower left refer to the linear regression coefficient (upper number) and the slope of the straight line fit (lower number, for highly linear fits).

(GL6P) levels. GL6PDH parameter changes affected GO6P without noticeably changing the RU5P pool concentrations. Decreasing V_{max} (GL6PDH) increased GO6P levels two fold. GO6P levels were insensitive to GL6PDH inhibition and equilibrium constants.

Of the enzymes explored, GSHR affected the greatest number of metabolite concentrations. Decreasing V_{max} (GSHR) decreased NADPH (increased $NADP^+$) by 60%, GL6P by 57%, RU5P by 15%, and erythrose 4-phosphate (E4P) by 20% while increasing GO6P by 30%. These widespread changes represented the indirect effect of changing NADPH levels on the activity of several enzymes.

TLC analysis for 10 h perturbations demonstrated few changes in metabolite pooling with these parameter changes. All major pools were consistent over each parameter change in PPP kinetics. Modal analysis, however, demonstrated significant differences. Decreased GSHR activity dissolved of one pair of imaginary time constants ($\tau = 0.14 \pm 0.01i$ h) into two real constants ($\tau = 0.14$ h, $\tau = 0.36$ h). This change represents a loss of underdamped, oscillatory behavior and certain dynamic features such as overshoot. S7P and E4P made up the largest contributors to the underlying modes. TLC analysis over the time scale of interest (0.74 h perturbations) showed GO6P correlated less strongly with G6P and F6P. HX and INO no longer showed strong correlation.

Phase planes were analyzed with a combination of ATP and redox loads for both the nominal and decreased V_{max} (GSHR) systems. Two time scales were selected to observe the impact of the changes in dynamics predicted by the modal analysis on the observed phase plane evolution of the concentration profiles. Fig. 2A shows the phase plane evolutions over time ranges from 0.05 h to 0.69 h, allowing the 0.14 h mode to approach steady-state. Fig. 2B shows the concentration phase plane evolutions over time ranges of 0.05 h to 1.81 h, allowing the 0.36 h mode to approach steady-state. Three significant differences were observed between the nominal and altered systems: GL6P levels changed relative to the other PPP metabolites; E4P moved on a slower time scale; and many of the slopes for consistent linear relations changed (see lower left corner, each panel Fig. 2), potentially indicating changes in the equilibrium relationships for the altered system. Nominally, GL6P levels decreased under the loads. Under the altered case, GL6P levels increased 5 fold from steady-state and GL6P pooled with the RU5P pool. The nominal case showed E4P levels increased initially as NADPH levels increased and then eventually decreased (Fig. 2A). The altered case did not demonstrate this behavior until a later time scale, as shown in Fig. 2B and predicted by the modal analysis. Both systems showed strong linear correlations. However, there were several slope changes. Decreased V_{max} (GSHR) showed GO6P changed with respect to $NADP^+$, GSH, and S7P with slopes of ~1/3 the nominal values. Other GSHR changes had less pronounced effects.

2.3 Transport Mechanisms

The four transport mechanisms explored affected the RBC steady-state differently (Tables I and IV). Of the three leaks, parameter changes in Na^+ leak had the most system-wide effect due to resulting effects on Na^+/K^+ ATPase activity which led, via propagation, to widespread ATP effects. When the Na^+ leak decreased (internal Na^+ decreased), less ATP was consumed exporting Na^+. HK became more active and increased both RU5P and PRPP (Table IV). When the Na^+ leak increased, ATP levels decreased less dramatically, although G6P levels decreased slightly. Major poolings from TLC analysis for the Na^+ leak showed that when the Na^+ leak increased ADE pooled negatively with pentose phosphate metabolites. This type of pooling was also observed in the analysis of HK parameter changes.

Two of the three Na^+/K^+ ATPase Pump inhibition constants significantly affected the system. Increasing $K_{m,Na+}$ caused intracellular K^+ levels to fall while intracellular Na^+, ATP and G6P levels increased. The Na^+/K^+ ATPase pump was not as interconnected with the rest of the cell as other systems in the RBC. In this model, intracellular levels of Na^+ and K^+ only affected levels of other metabolites through the ATP required for the pump. When pump activity decreased, intracellular Na^+ increased and the additional ATP phosphorylated more glucose. Levels of other metabolites did not change significantly.

2.4 Adenosine Metabolism

Three key adenosine metabolism enzymes were analyzed: adenylate kinase (ADK), ATP phosphohydrolase (ATPase), and AMP phosphohydrolase (AMPase). Parameter changes in each of these enzymes demonstrated sensitivity. In particular changes in the ATPase parameters (Ψ^-=4.54, Ψ^+=4.00) influenced several RBC metabolite levels.

Decreased ATPase activity corresponded to a decreased glycolytic flux, leading to build up of the early glycolytic and PPP metabolites, including G6P, ADP, RU5P, PRPP, and NADPH. Modal analysis showed the loss of the pair of complex conjugate modes (τ=0.14 ± 0.01*i* h) to (τ=0.21 h, τ=0.16 h). Phase plane analysis comparing the nominal system to decreased ATPase activity over the time scale of 0.5-1.5 h showed a dramatic change in the dynamics of NADH. Over this time scale, NADH was nominally linear ($r^2 \approx 0.96$) with all other metabolites, but highly nonlinear in the case of the ATPase altered case. TLC analysis for perturbations every 0.21 h showed few differences between the systems except in the correlation between HX and INO. The maximum correlation between the two was 0.96 for the nominal case and 0.77 in the altered ATPase case. A similar trend was seen for many of the parameter changes studied. TLC analysis with 10 h perturbations did not show significant differences between the nominal and altered ATPase system.

Other parameter changes showed slight pooling changes. Decreased V_{max} (AMPase) and an ADK equilibrium shift towards ATP gave similar pooling due to net decreases in the concentrations of the glycolytic species. Shifting ADK equilibrium towards ATP/AMP caused levels of ADP, ATP and G6P to drop. Levels of DPG13, DPG23, fructose-1,6-bisphosphate (FDP) and $NADP^+$ increased. This behavior was examined through a flux analysis of the kinetic expressions. Under deficits in ADP, a larger fraction of the flux passed through the Rapoport-Leubering bypass and less ADP was used. However, this also caused ATP levels to decrease because a generation step was bypassed. Alternatively, decreasing AMPase activity led to unique behavior not seen by the other parameter changes explored. G6P and ADO levels decreased while AMP, ADP, and ATP levels increased.

3. Discussion

The most sensitive enzymatic parameters explored were V_{max} (HK) (Ψ^-=11.11, Ψ^+=10.00), G6PDH equilibrium (Ψ^-=9.10, Ψ^+=8.33), and V_{max} (ATPase) (Ψ^-=4.54, Ψ^+=4.00). Each of these significantly changed the steady-state of most metabolites in the system. Conversely, many parameter alterations only affected a few metabolite levels. In general, the model was sensitive to equilibrium constants for reversible reactions and relatively insensitive to inhibition constants.

An unexpected trend of the system occurred when HK was more active due to parameter changes resulting in increased overall ATP in the cell. In these cases, PRPP and the RU5P pool rose more than other metabolites. Nominally, ADE transport appeared limiting relative to PRPP production in the formation of AMP. This was not the case in systems with decreased ATP levels. Analysis of several parameter changes concluded that increased levels of the RU5P pool indicated increased fluxes through either PPP or glycolysis. GL6P is well-regulated and only directly affected by changes in the regulation by $NADP^+$.

Each method studied possessed distinct advantages and disadvantages. TLC depended on the frequencies of perturbation and measurement. With 10 h perturbations, only the most sensitive parameter changes caused new poolings. Generally, TLC offered more information than either of the other two analyses studied. However, as TLC analysis was more involved, it was helpful when suitable time scales for perturbing the system were known. The major TLC poolings revealed that most parameter alterations resulted in one or two pooling changes. Many of these changes represented moderate differences in correlation, indicating strong interaction was still present. In the nominal case, the correlations between HX, INO, and ADO were very strong, but in most of the perturbed cases studied, $r_{ij} \leq 0.5$. These metabolites were not as tightly controlled with respect to one another as other RBC poolings. This needs to be explored further as it may provide potential insight into the RBC model. GL6P never correlated strongly with GO6P, indicating distinct

regulation of the metabolites. TLC provided insight into interconnectivity between pools and how those connections changed in response to parameter changes. However, a priori identification of interesting time scales was helpful.

Modal analysis revealed time scale sensitivity to network parameter changes. Single parameter alterations typically caused significant changes in one or two time constants while the other time scales remained the same. Imaginary pairs of modes tended to show more interesting behavior: the addition or subtraction of a pair indicated significant dynamic changes. Analysis of the modes of the system determined where and how system dynamics changed with respect to the nominal system. Phase planes constructed for these regions, gave insight into the specific dynamic changes that occurred as a result of changing the parameters. For cases where a full model is not available, phase plane analysis could be used to identify the time scale where differences are most apparent. These differences could then be characterized more fully with either additional phase plane or TLC analyses.

These analyses demonstrate that common systems techniques are able to identify differences in metabolic networks that result from changes in single parameters. Although not presented here, introducing noise up to four percent into the system for time-lagged correlation analysis produced similar maximum correlation results, even though the peaks were not as pronounced. Using triplicate measurements effectively halved the effect of noise. The changes studied are representative of various pathological conditions such as infections, genetic variability, and environmental effects. Analyses such as this also provide insight into how several distinct pathological conditions can give rise to the same phenotypic symptoms.

4. Conclusions

Each of the analyses offered useful insight into cellular regulation. Modal analysis was most constructive as a starting point to determine the time scales on which alterations manifested. These time scales were then studied further with phase planes and correlation analysis. Rarely did more than one or two of the 34 time scales change in the modal analysis for the parameter changes observed. Phase planes identified major dynamic differences including changes in relationships. Phase planes visually demonstrated time scale differences manifestations better than either of the other techniques. As a result, phase planes could potentially be used to identify time scales of interest when modal analysis wasn't available due to lack of a complete model. TLC provided insight into changes in interaction and was better suited to decompose effects than phase plane analysis. A priori identification of the most significant time scale enhanced the utility of TLC. TLC showed subtle pooling differences under parameter changes, even though the analysis was more complex. Further work is needed to classify system responses for each possible single parameter alteration, explore the effects of multiple parameter alterations, examine

changes to the fundamental kinetics of the system, and explore scalability issues regarding the sensitivity and utility of TLC, phase plane, and modal analyses.

Acknowledgements

Financial support was provided in part by a NASA Graduate Student Researcher's Program Fellowship (KJK, NGT5-50367), NIH BRIN Fellowship (REA, 1P20 RR16472-01) and NIH Grant 5P20 RR15588-02.

References

1. A. Joshi, B. O. Palsson, "Metabolic dynamics in the human red cell. Part I--A comprehensive kinetic model." *J Theor Biol* **141**, 515 (1989).
2. A. Joshi, B. O. Palsson, "Metabolic dynamics in the human red cell. Part II--Interactions with the environment." *J Theor Biol* **141**, 529 (1989).
3. A. Joshi, B. O. Palsson, "Metabolic dynamics in the human red cell. Part III--Metabolic reaction rates." *J Theor Biol* **142**, 41 (1990).
4. A. Joshi, B. O. Palsson, "Metabolic dynamics in the human red cell. Part IV--Data prediction and some model computations." *J Theor Biol* **142**, 69 (1990).
5. J. Edwards, B. Palsson, "Multiple steady states in kinetic models of red cell metabolism." *J Theor Biol* (2000).
6. N. Jamshidi, J. S. Edwards, T. Fahland, G. M. Church, B. O. Palsson, "Dynamic simulation of the human red blood cell metabolic network." *Bioinformatics* **17**, 286 (2001).
7. D. Fell, *Understanding the Control of Metabolism* (Portland Press, London, 1996).
8. A. Arkin, J. Ross, "Statistical Construction of Chemical Reaction Mechanisms From Measured Time-Series." *J Phys Chem* **99**, 970 (1995).
9. A. Arkin, P. D. Shen, J. Ross, "A test case of correlation metric construction of a reaction pathway from measurements." *Science* **277**, 1275 (1997).
10. K. J. Kauffman, J. D. Pajerowski, N. Jamashidi, B. O. Palsson, J. S. Edwards, "Description and Analysis of Metabolic Connectivity and Dynamics in the Human Red Blood Cell." *Biophys J* **83**, 646 (2002).
11. "FORTRAN Library Documentation, Mark 20" (Numerical Algorithms Group, 2002, pp. D02NDF.1).
12. J. Hubbard, B. H. West, *Differential equations: a dynamical systems approach*, Texts in applied mathematics; 5,18 (Springer-Verlag, New York, 1991).
13. A. Varma, M. Morbidelli, *Mathematical Methods in Chemical Engineering* (Oxford University Press, New York, 1997).